NPA8 2017 Catania

Measurements of the ^{20}Ne+α resonant elastic scattering for characterization of the ^{24}Mg states at relevant excitations for carbon - carbon burning proces

Neven Soić, Ruđer Bošković Institute, Zagreb, Croatia

Collaborators

1) V. Tokić, T. Mijatović, L. Prepolec, N. Skukan, S. Szilner, M. Uroić
Ruđer Bošković Institute, Zagreb, Croatia
2) M. Milin
Faculty of Science, University of Zagreb, Zagreb, Croatia
3) J. P. Fernandez Garcia, P. Figuera, M. Fisichella, M. Lattuada
LNS-INFN/University of Catania, Catania, Italy
4) S. Bailey, R. Smith, J. Walshe
University of Birmingham, Birmingham, United Kingdom
5) L. Acosta, I. Martel, G. Marquinez-Duran
University of Huelva, Huelva, Spain
6) E. Fioretto
LNL-INFN, Padova, Italy

Motivation

- Objective: search for $^{12}C+^{12}C$ resonances at the ^{24}Mg excitations 15-18 MeV and their full characterization: excitation energy, width, spin, parity, partial decay widths
- Two-fold reason: nuclear structure & astrophysical motivation

Important new result is even observation of the 0^+ or 1^- state at these excitations with prominent cluster structure but not exclusively decaying into $\alpha+^{20}Ne$

20 MeV

$E_{thr}(n+^{23}Ne) = 16.532$ MeV

$E_{thr}(\alpha+\alpha+^{16}O) = 14.044$ MeV

$E_{thr}(^{12}C+^{12}C) = 13.931$ MeV

$E_{thr}(^{1}H+^{23}Na) = 11.692$ MeV

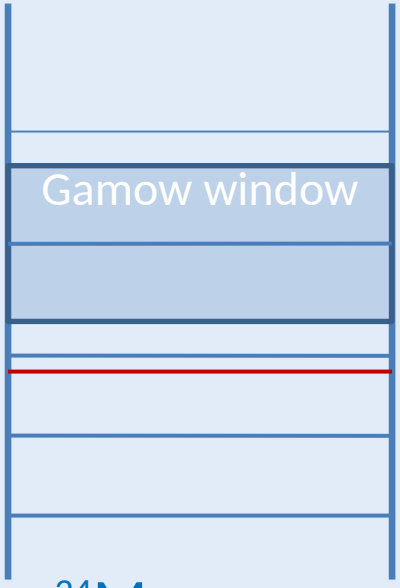

$E_{thr}(\alpha+^{20}Ne) =$

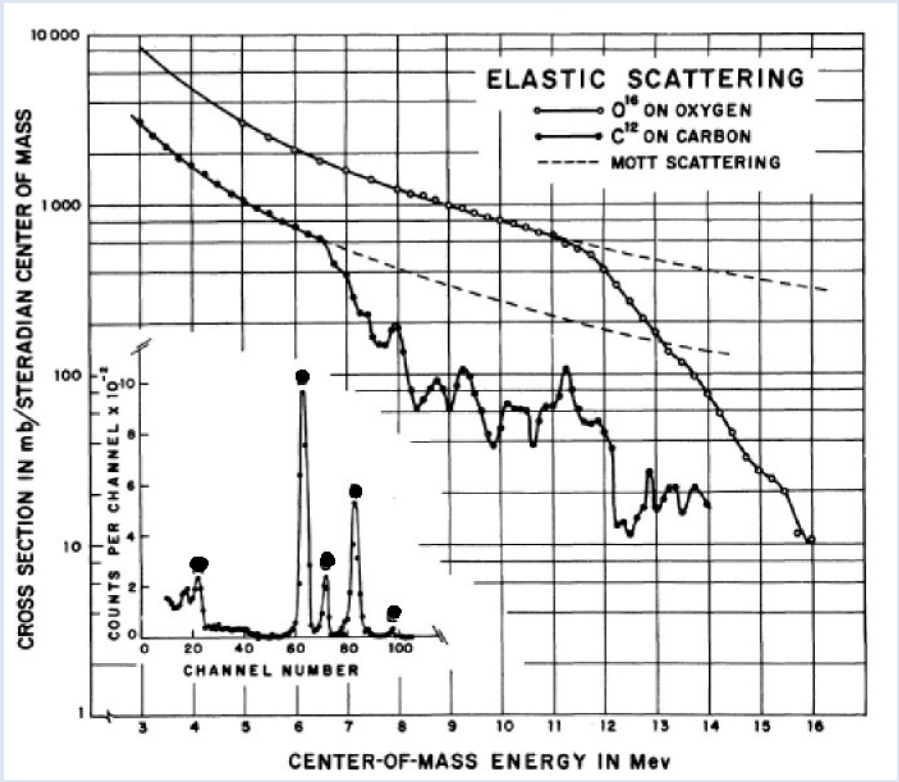

Elastic scattering data
D. A. Bromley, J. A. Kuehner, E. Almquist, Phys..Rev. Lett. 4 (1960) 385

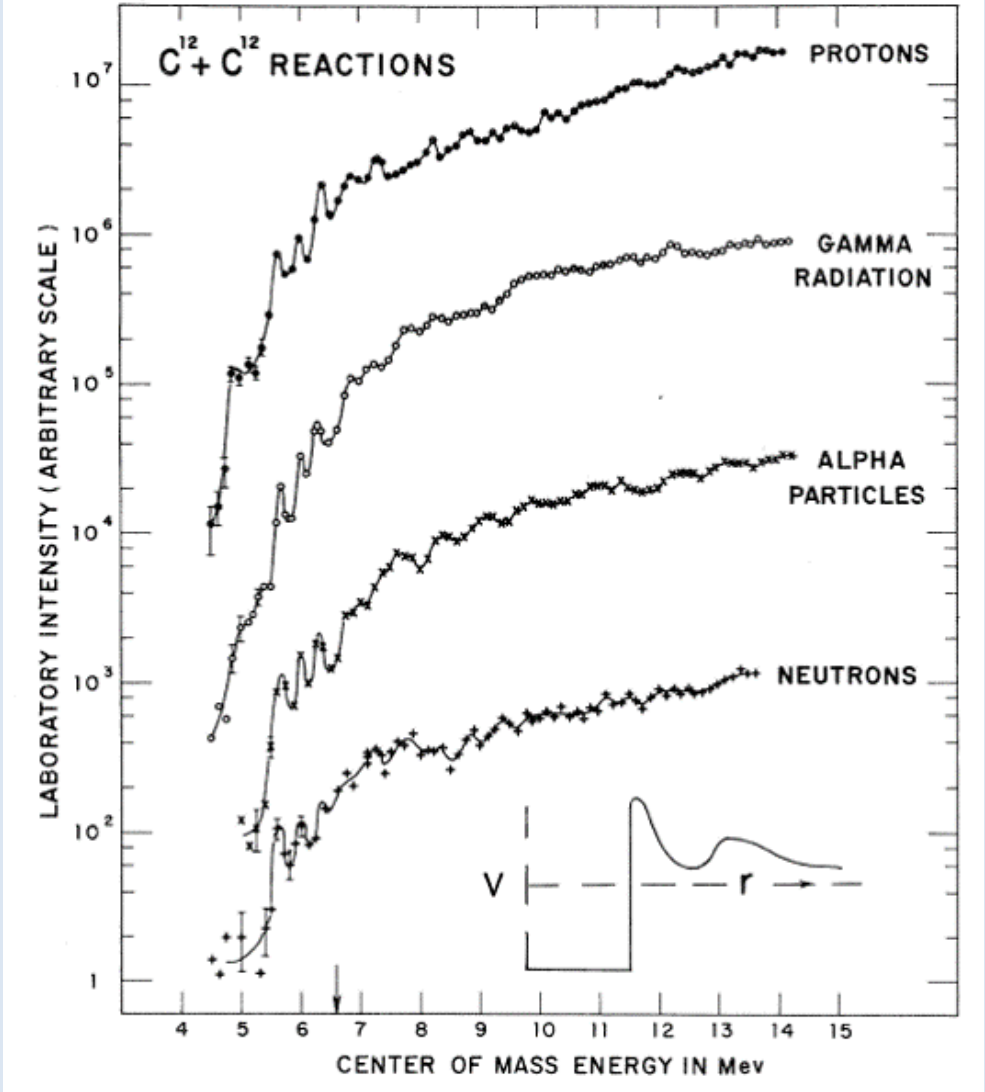

Reaction data
E. Almquist, D. A.Bromley, J. A. Kuehner, Phys. Rev. Lett. 4 (1960) 515

Formation of quasi-molecular states in ^{24}Mg

B. R. Fulton et al, Phys Lett B 267 (1991) 325

M. Freer et al, Phys Rev C 57 (1998) 1277
C. Metelko et al, Phys Rev C 68 (2003) 054321

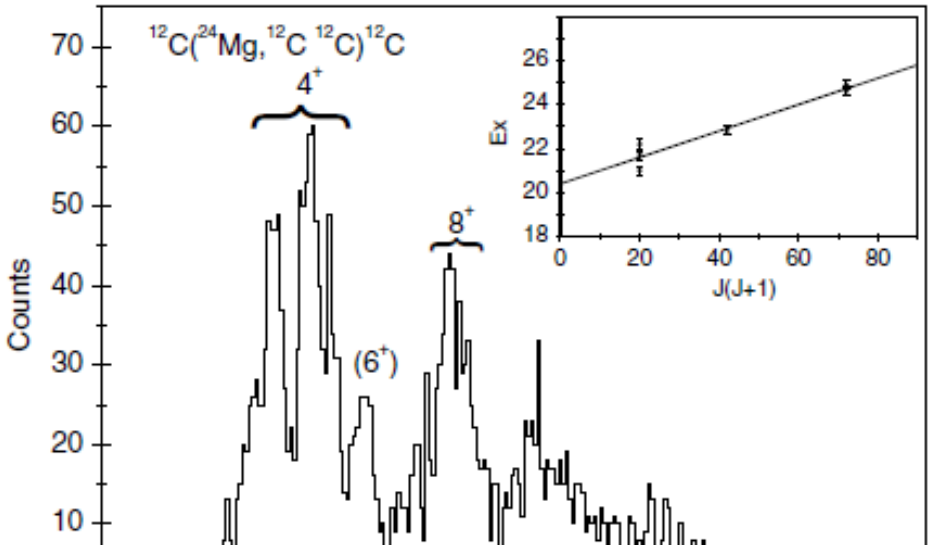

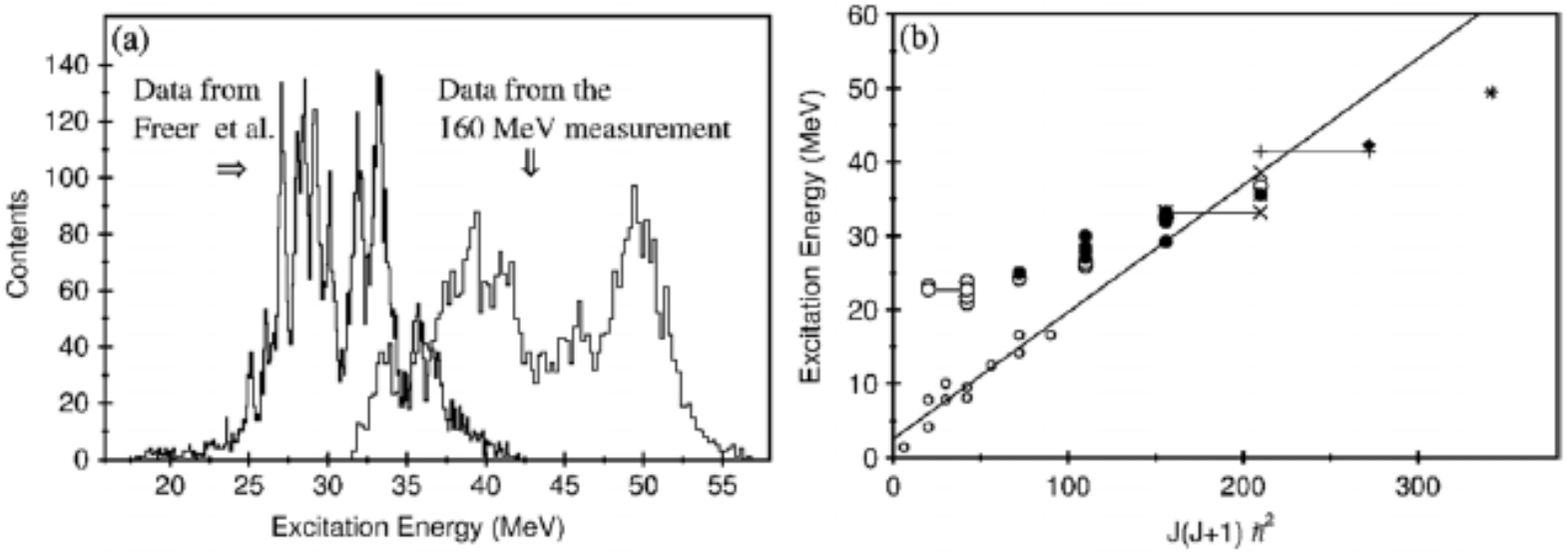

Figure 42. (*a*) Resonances observed in the $^{12}C(^{16}O,^{24}Mg^*)$ breakup reaction [147, 148]. (*b*) The energy-spin systematics of the breakup resonances, from [148]. The smaller symbols and the solid line indicates the trend of the yrast states in ^{24}Mg.

T. Kawabata et al,
J. Phys. Conf. Ser. 436, 012009 (2013)

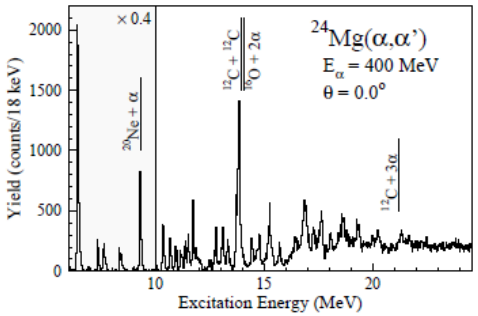

Figure 1. Typical spectrum for the ^{24}Mg(α,α') reaction measured at 0°. The excitation spectrum below $E_x = 10$ MeV is downscaled by a factor of 0.4.

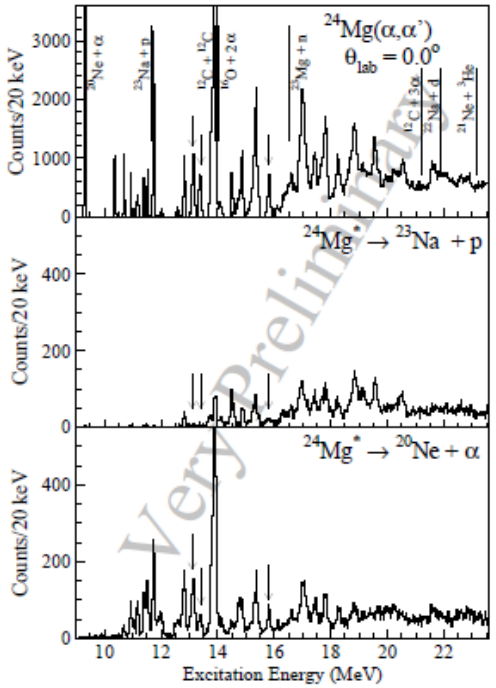

Figure 4. Excitation energy spectra in the ^{24}Mg(α,α') reaction at E_x = 9–23.6 MeV taken from the singles measurement (top) and from the coincidence measurements with decay protons (middle) and α particles (bottom). The vertical arrows show the 0^+ states at 13.1, 13.4, and 15.8 MeV.

The 13.1, 13.4 and 15.8 MeV states have prominent α-cluster structure

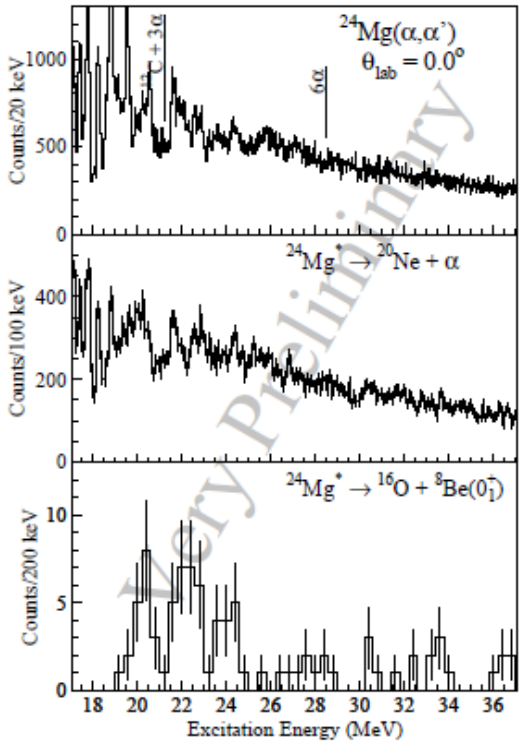

Figure 5. Excitation energy spectra in the ^{24}Mg(α,α') reaction at E_x = 17.1–37.1 MeV taken from the singles measurement (top) and from the coincidence measurements with decay α particles (middle) and ^{8}Be (bottom).

- Y. Chiba and M. Kimura, PRC 91, 061302(R) (2015)
- antisymmetrized molecular dynamics combined with the generator coordinate method

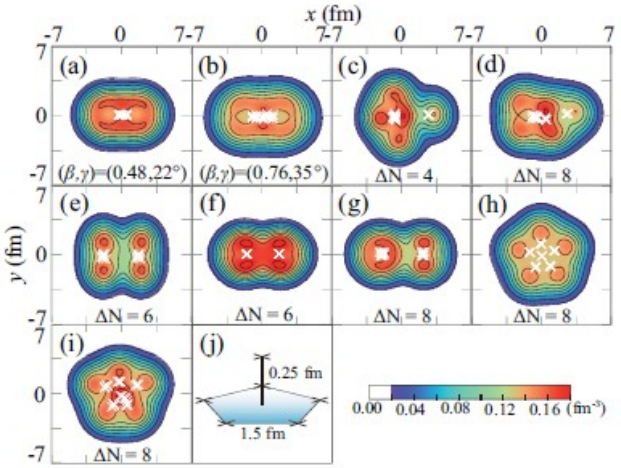

FIG. 1. (Color online) (a)–(i) Intrinsic density distributions at the $z = 0$ plane obtained by constraints on the matter quadrupole deformation parameters [(a) and (b)] and the expectation values of the harmonic oscillator quanta [(c)–(i)]. The crosses in each figure show the centroids of Gaussians describing nucleons. The contour lines are plotted in intervals of 0.02 fm^{-3}. (j) The geometry of 6α particles, in which the crosses represent the centroids of Gaussians describing α particles.

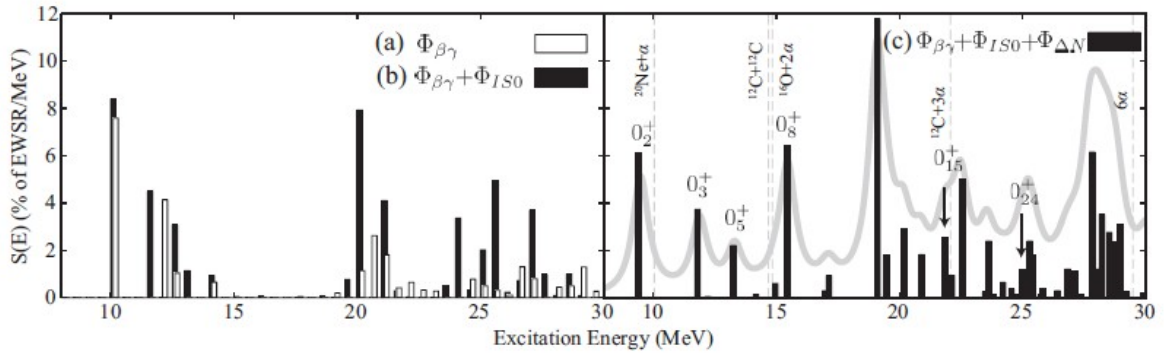

FIG. 2. The isoscalar monopole transition strength functions calculated with the basis sets (a) $\Phi_{\beta\gamma}$, (b) $\Phi_{\beta\gamma} + \Phi_{IS0}$, and (c) $\Phi_{\beta\gamma} + \Phi_{IS0} + \Phi_{\Delta N}$. The solid line in the right panel shows the strength function smeared by a Lorentzian with 0.8 MeV width. The vertical dashed lines indicate cluster decay threshold energies which are located at the observed binding energies.

The ^{24}Mg ground state has significant cluster components ^{4}He+^{20}Ne and ^{12}C+^{12}C
The ^{12}C+^{12}C configuration contributes to the O_2^+, O_3^+, O_5^+, and is the main component of the O_8^+ state at 15.3 MeV

SNIa: 0.5 - 1.2x10^9 K → E_{cm}=1.5-3.3 MeV → 15.4 – 17.2 MeV

Super-bursts: trigger of ^{12}C ignition up to 2.5x10^9 K → 5.7 MeV

Massive stars: ^{12}C+^{12}C fusion - white dwarf or heavy elements burning

Super-AGB stars

Relevant reactions: $^{12}C + {}^{12}C \rightarrow {}^{20}Ne + \alpha$, Q=4.617 MeV

$^{12}C + {}^{12}C \rightarrow {}^{23}Na + p$, Q=2.239 MeV

E. F. Aguilera et al, Phys. Rev. C 73 (2006) 064601

T. Spillane et al, Phys. Rev. Lett. 98 (2007) 122501

V. Yu. Denisov and N. A. Pilipenko, Phys. Rev. C 81 025805 (2010)

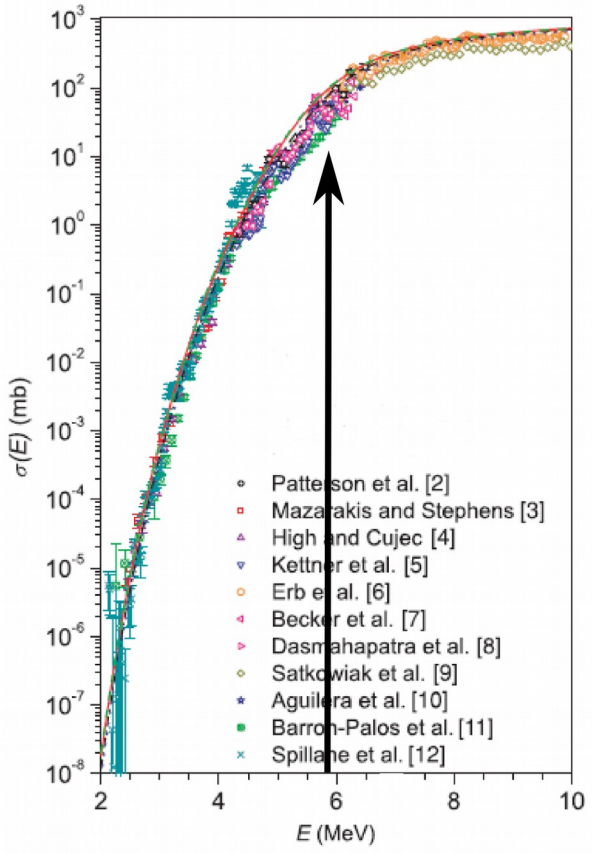

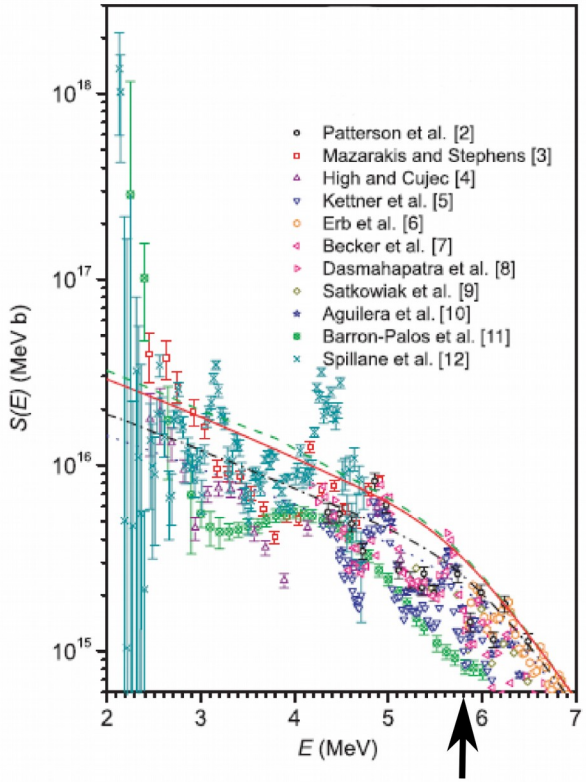

Experiment at INFN – LNS

Coincident detection of 2 (or more) reaction products

$^{12}C + {}^{16}O \rightarrow {}^{4}He + {}^{12}C + {}^{12}C$ Q=-7.16 MeV $E_{thr}(^{24}Mg)$=13.93 MeV

$\rightarrow {}^{4}He + {}^{16}O + {}^{8}Be$ Q=-7.37 MeV $E_{thr}(^{24}Mg)$= 14.14 MeV

$\rightarrow {}^{4}He + {}^{20}Ne + {}^{4}He$ Q=-2.54 MeV $E_{thr}(^{24}Mg)$= 9.31 MeV

$\rightarrow {}^{4}He + {}^{23}Na + {}^{1}H$ Q=-4.92 MeV $E_{thr}(^{24}Mg)$= 11.69 MeV

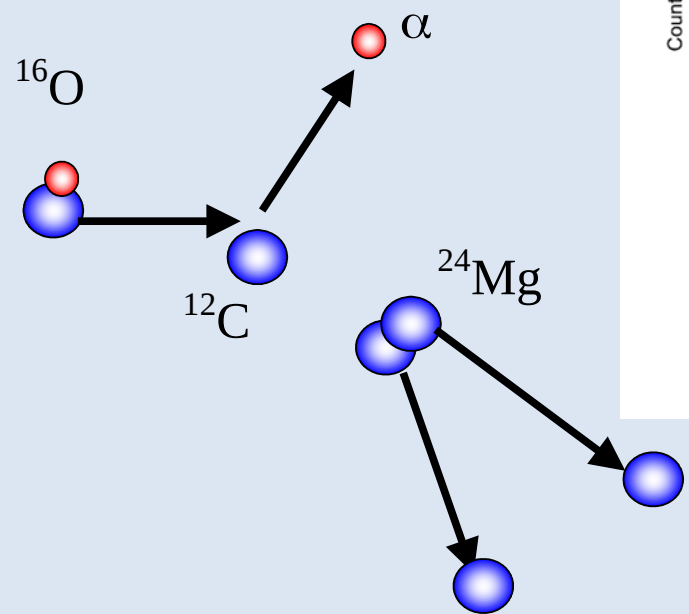

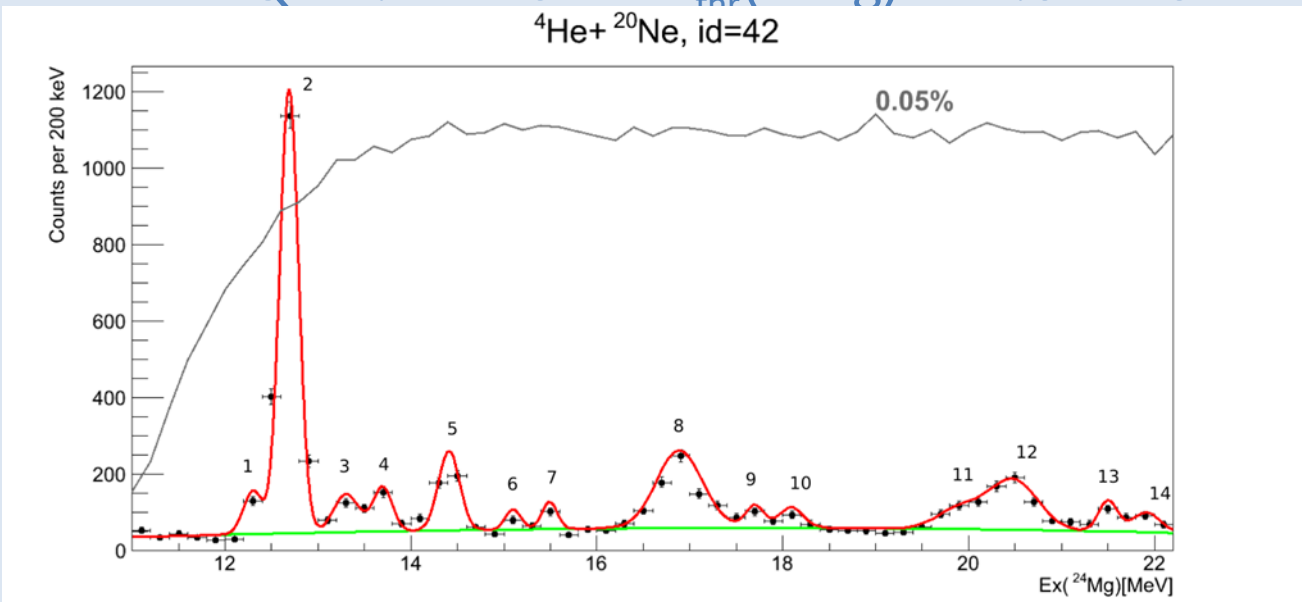

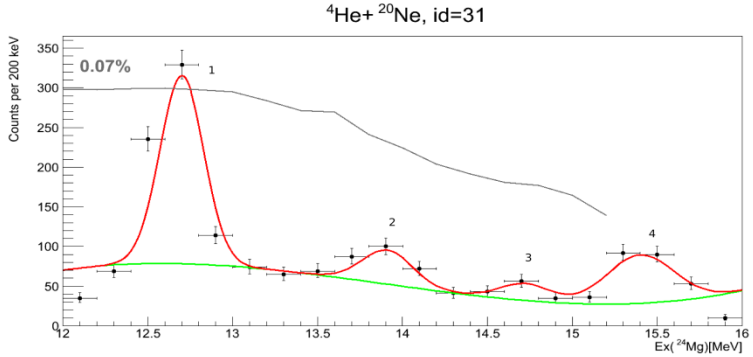
^{4}He+ ^{20}Ne, id=31
0.07%
Counts per 200 keV
Ex(^{24}Mg)[MeV]

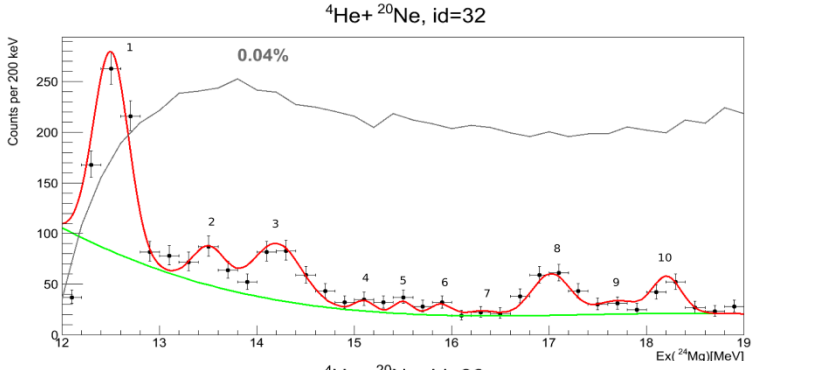
^{4}He+ ^{20}Ne, id=32
0.04%
Counts per 200 keV
Ex(^{24}Mg)[MeV]

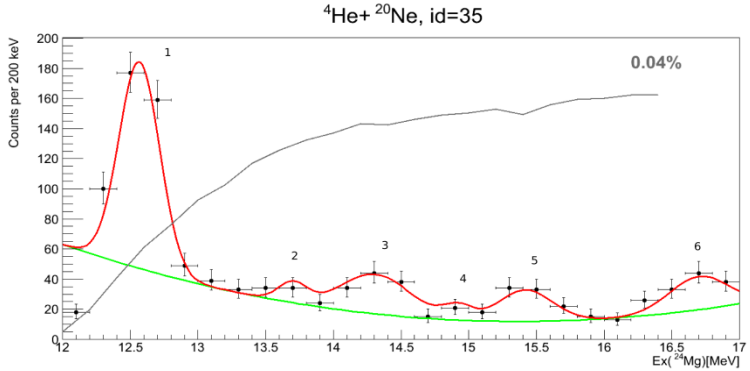
^{4}He+ ^{20}Ne, id=35
0.04%
Counts per 200 keV
Ex(^{24}Mg)[MeV]

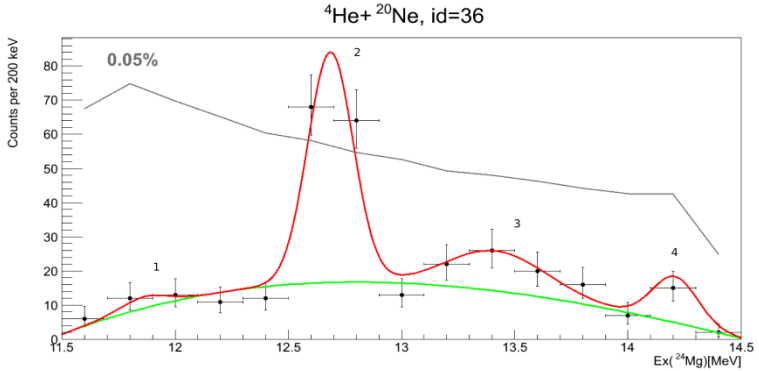
^{4}He+ ^{20}Ne, id=36
0.05%
Counts per 200 keV
Ex(^{24}Mg)[MeV]

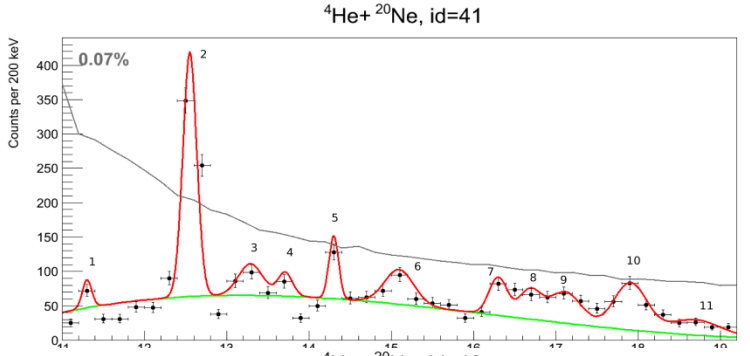
^{4}He+ ^{20}Ne, id=41
0.07%
Counts per 200 keV

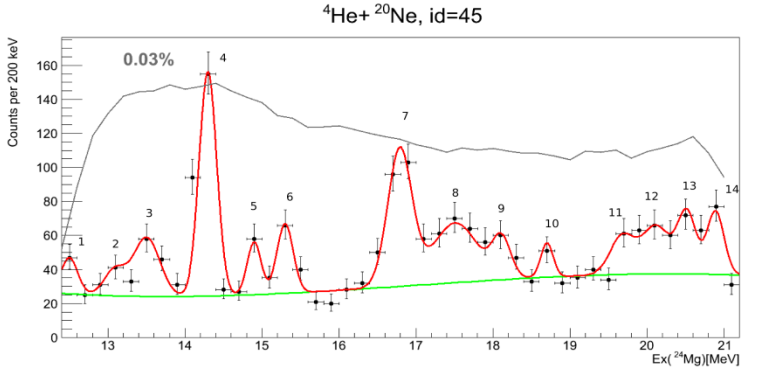
^{4}He+ ^{20}Ne, id=45
0.03%
Counts per 200 keV
Ex(^{24}Mg)[MeV]

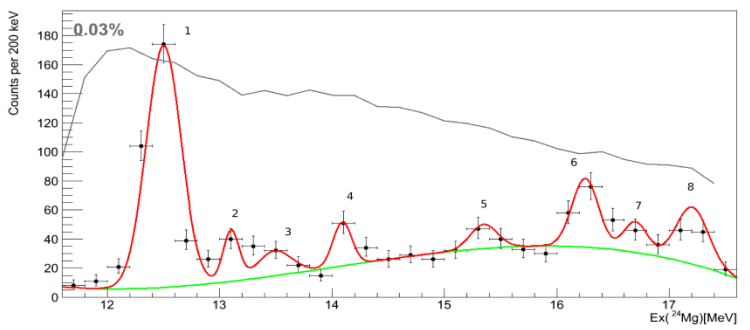
^{4}He+ ^{20}Ne, id=46
0.03%
Counts per 200 keV
Ex(^{24}Mg)[MeV]

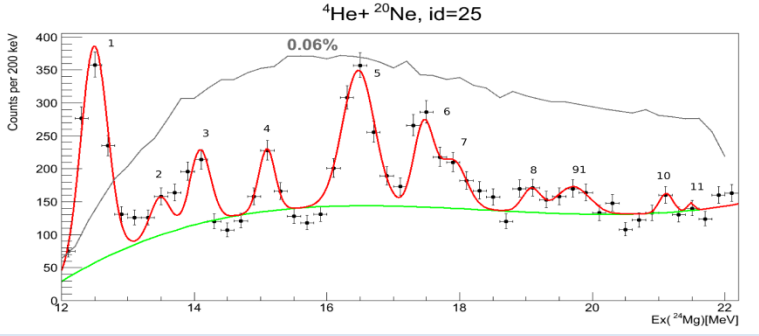
^{4}He+ ^{20}Ne, id=25
0.06%
Counts per 200 keV
Ex(^{24}Mg)[MeV]

- $^{12}C(^{16}O,\alpha\alpha)^{20}Ne^{*}$ $^{12}C(^{16}O,\alpha\alpha)^{20}Ne^{**}$

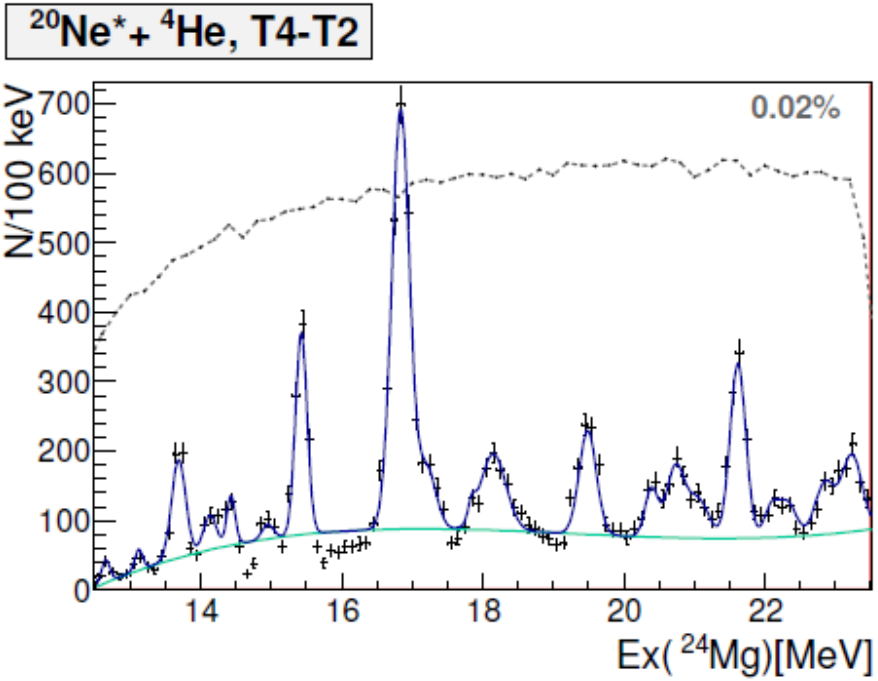

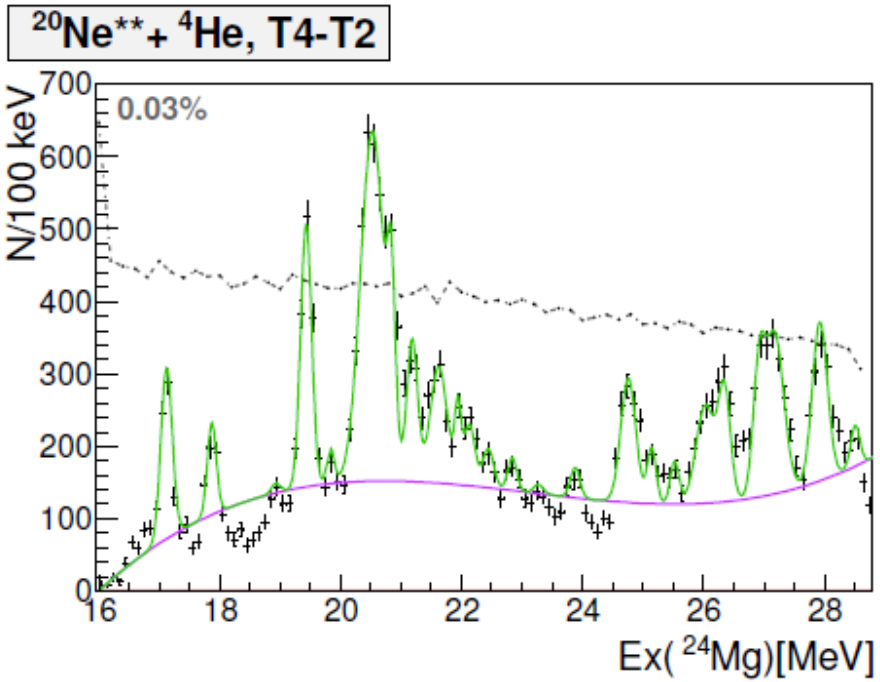

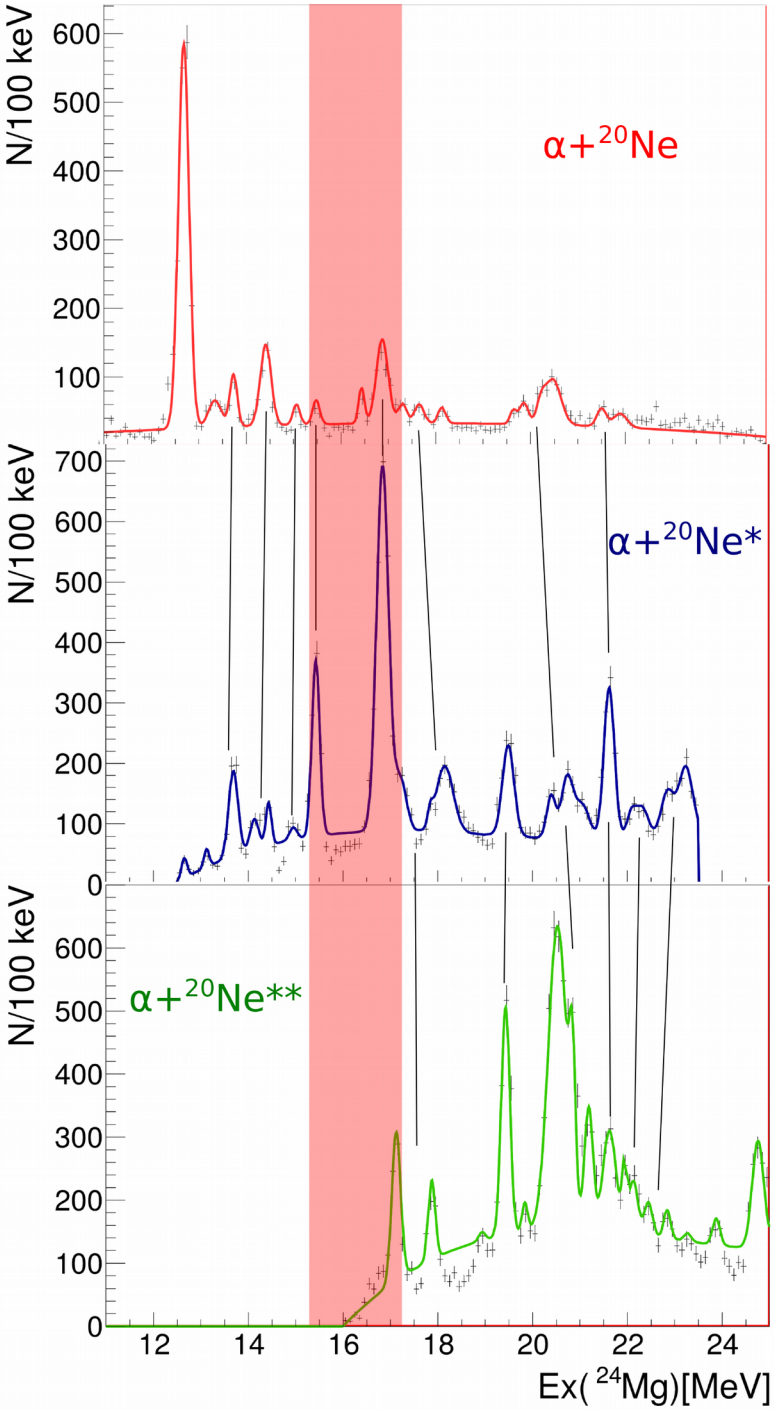

- detected ^{24}Mg states decaying into ^{20}Ne gs (0^+), 1st (2^+) and 2nd (4^+) excited state
- branching ratio for some of the states
- prefered decay into excited state → high spin states
- no evidence for any 0^+ or 1^- state

^{20}Ne+α resonant scattering experiment

thick gas target exp: ΔE-E telescope at 0 deg

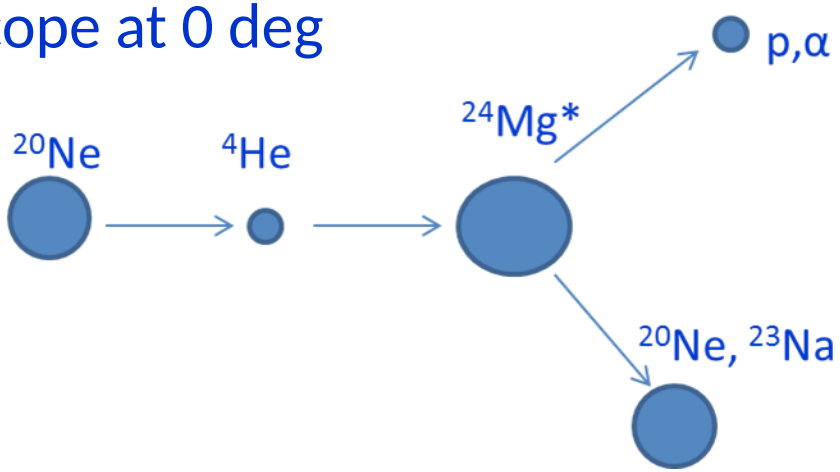

The ^{24} Mg excitation energy spectra from α's in the telescope

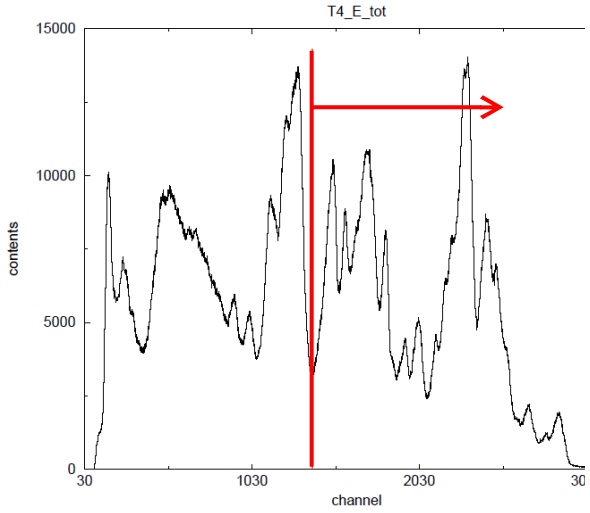

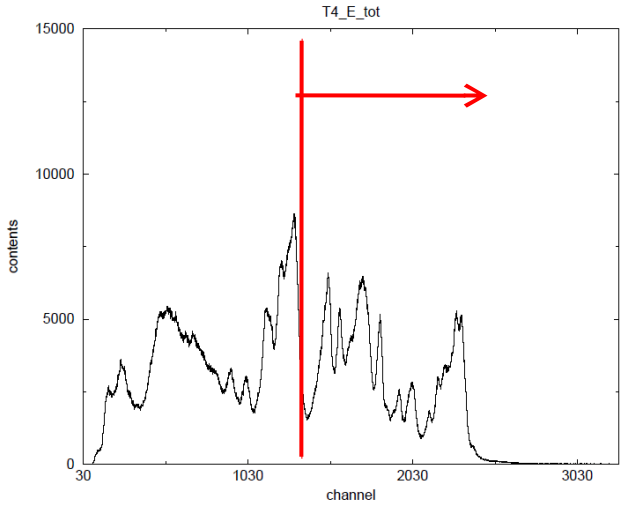

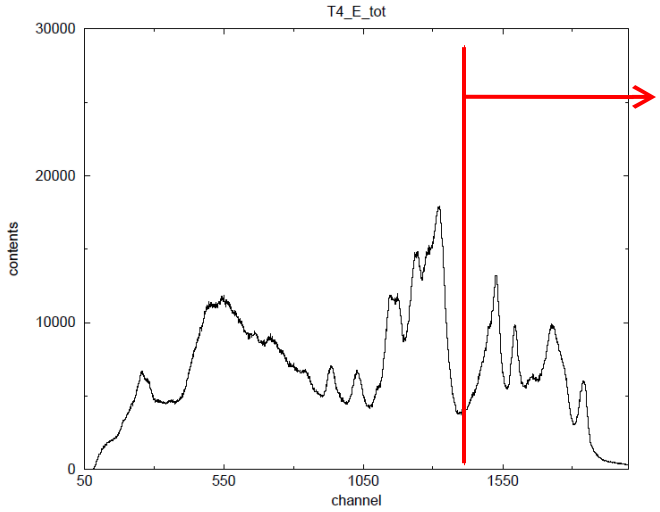

Beam energy

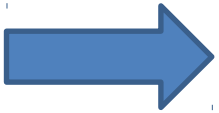

Spectra for all pixels together

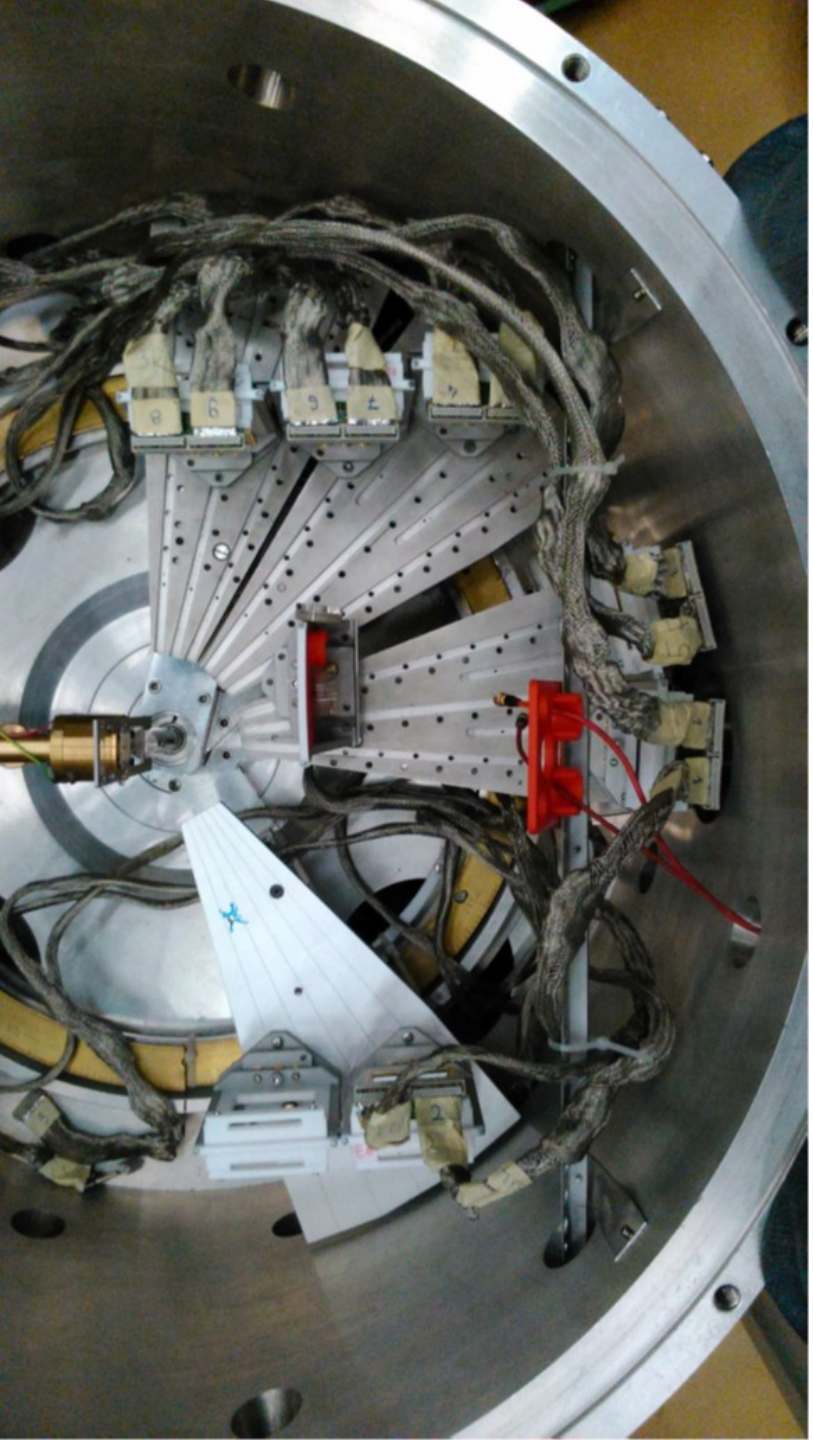

INFN - LNL Legnaro 2014

^{20}Ne beam from PIAVE + ALPI facility

LIRAS chamber

- entrance window: 2μm HAVAR foil
- ^{4}He gas target pressure up to 800 mbar
- beam stopped before the 0^{o} telescope

- side detectors: scattered α's have low energy + energy loss and straggling in the gas – unresolved resonances

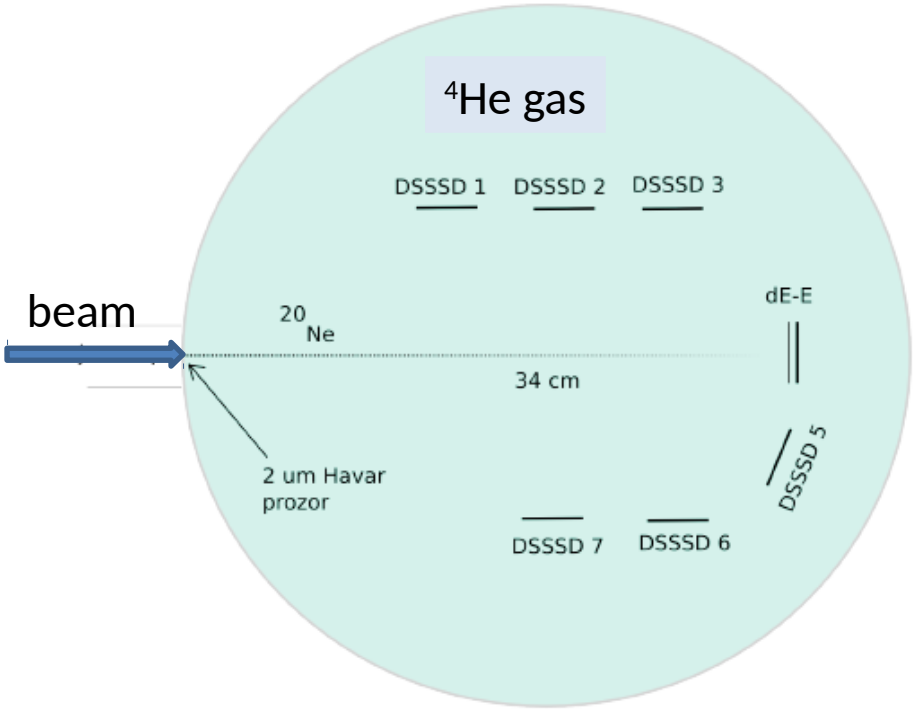

- from energy and angle of the detected α calculated ^{24}Mg excitation energy

$E_x(^{24}Mg)$ vs $\theta_{CM}(\alpha)$ for Zero degree telescope data

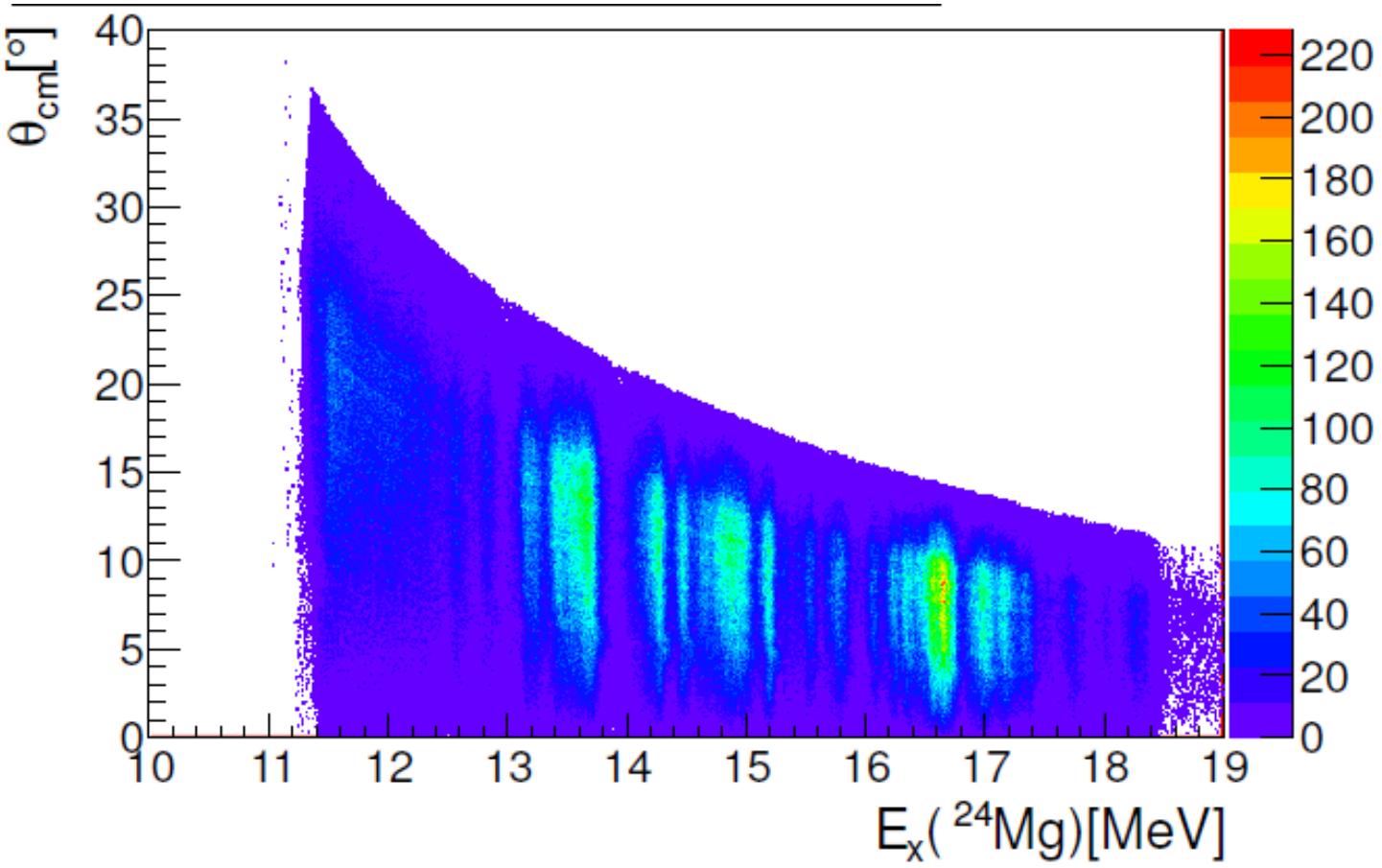

Detector telescope at 0 degree: normalized to previous GANIL measurements and efficiency corrected (±5°) data for three beam energies ($\theta_{CM}(^{24}Mg)=177^{o}$)

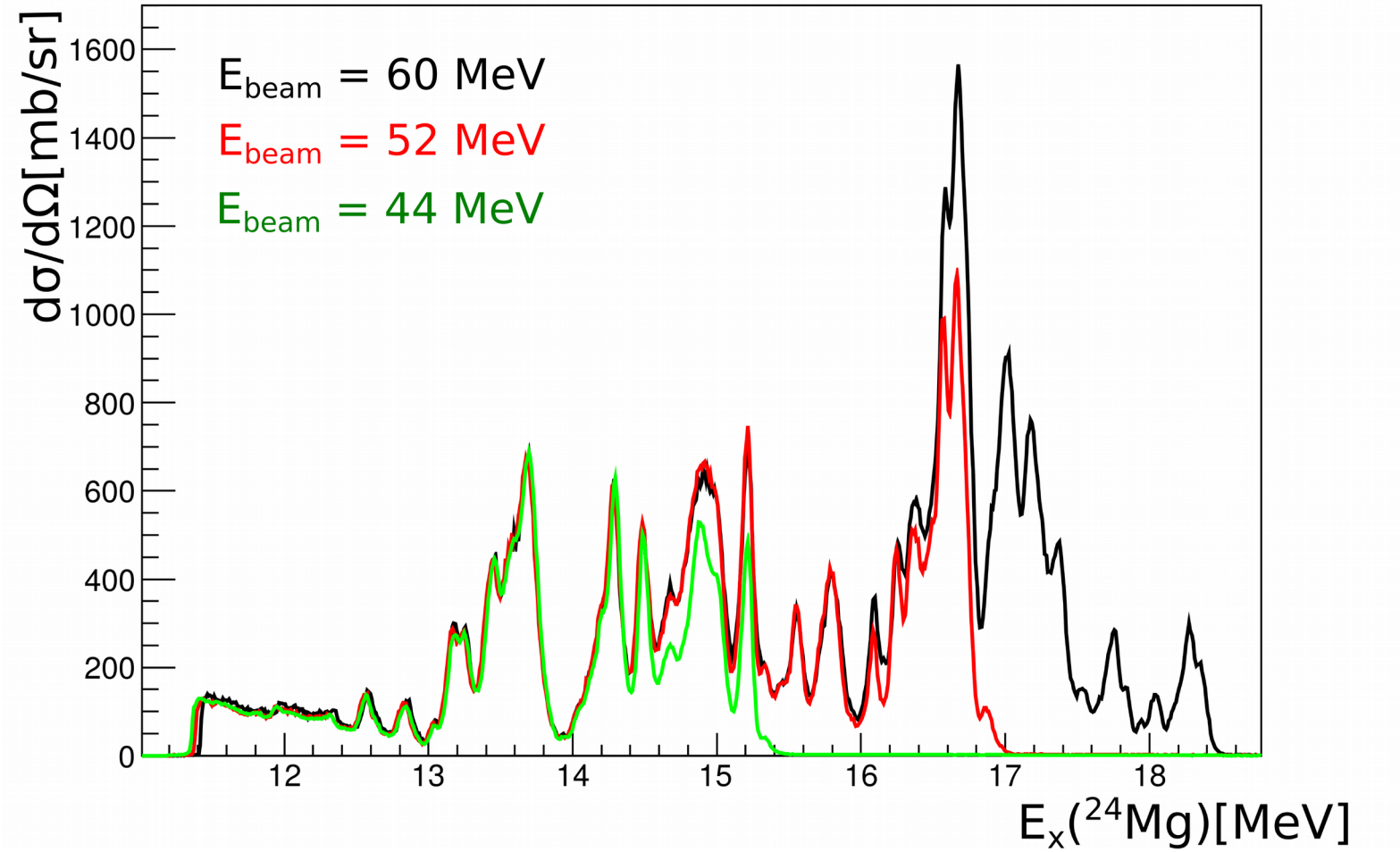

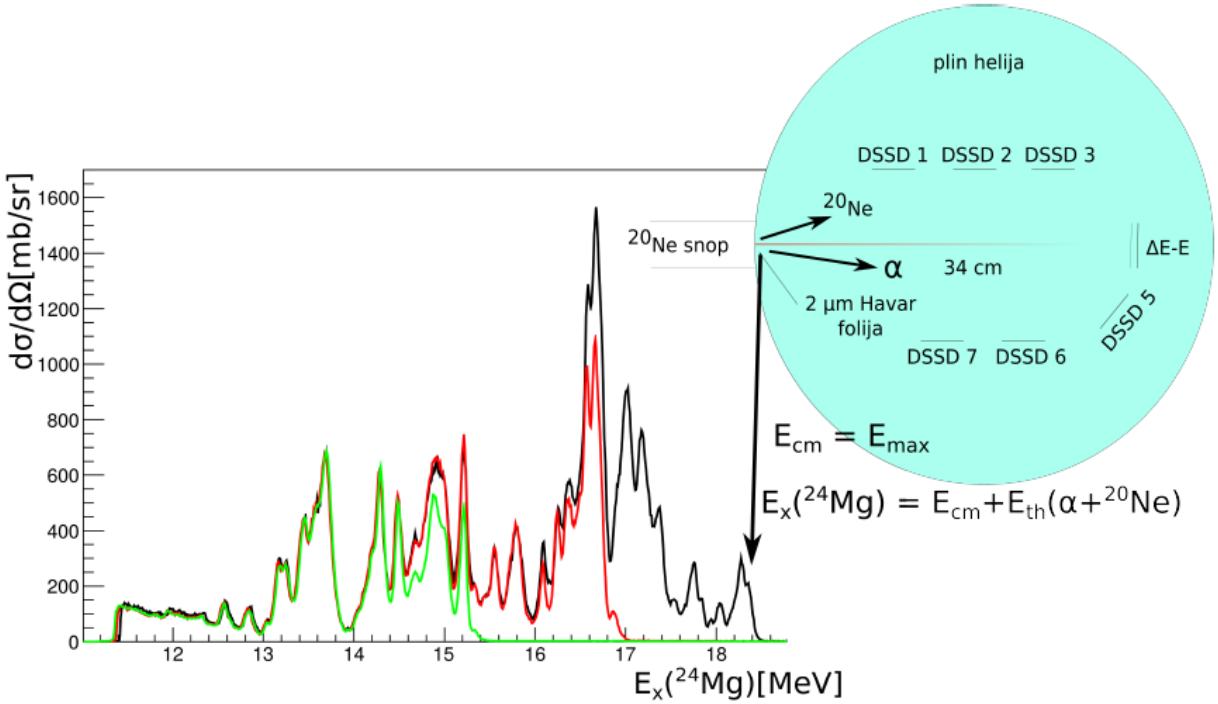
plin helija
DSSD 1 DSSD 2 DSSD 3
^{20}Ne
α
34 cm
ΔE-E
2 μm Havar folija
DSSD 5
DSSD 7 DSSD 6
^{20}Ne snop
$E_{cm} = E_{max}$
$E_x(^{24}Mg) = E_{cm}+E_{th}(\alpha+^{20}Ne)$
dσ/dΩ[mb/sr]
$E_x(^{24}Mg)$[MeV]

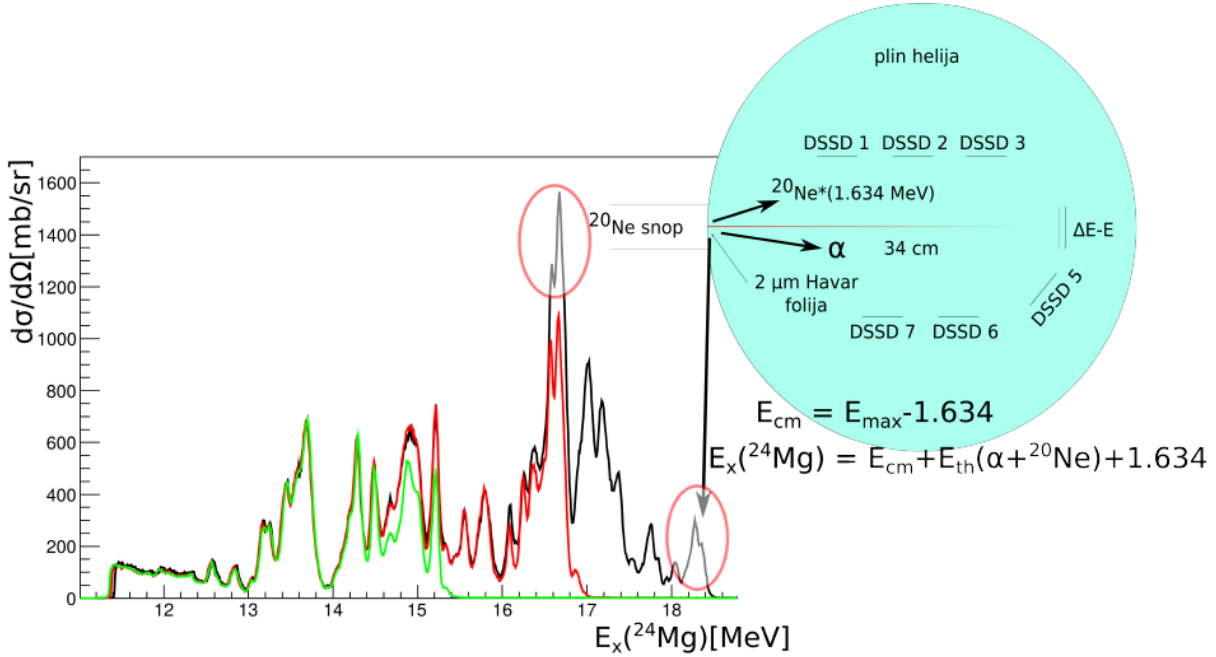
plin helija
DSSD 1 DSSD 2 DSSD 3
^{20}Ne*(1.634 MeV)
α
34 cm
ΔE-E
2 μm Havar folija
DSSD 5
DSSD 7 DSSD 6
^{20}Ne snop
$E_{cm} = E_{max}$-1.634
$E_x(^{24}Mg) = E_{cm}+E_{th}(\alpha+^{20}Ne)+1.634$
dσ/dΩ[mb/sr]
$E_x(^{24}Mg)$[MeV]

Coloured windows mark part of the excitation energy spectrum free from inelastic contribution for three beam energies

$E_{cm}=E_{max}-E_x$

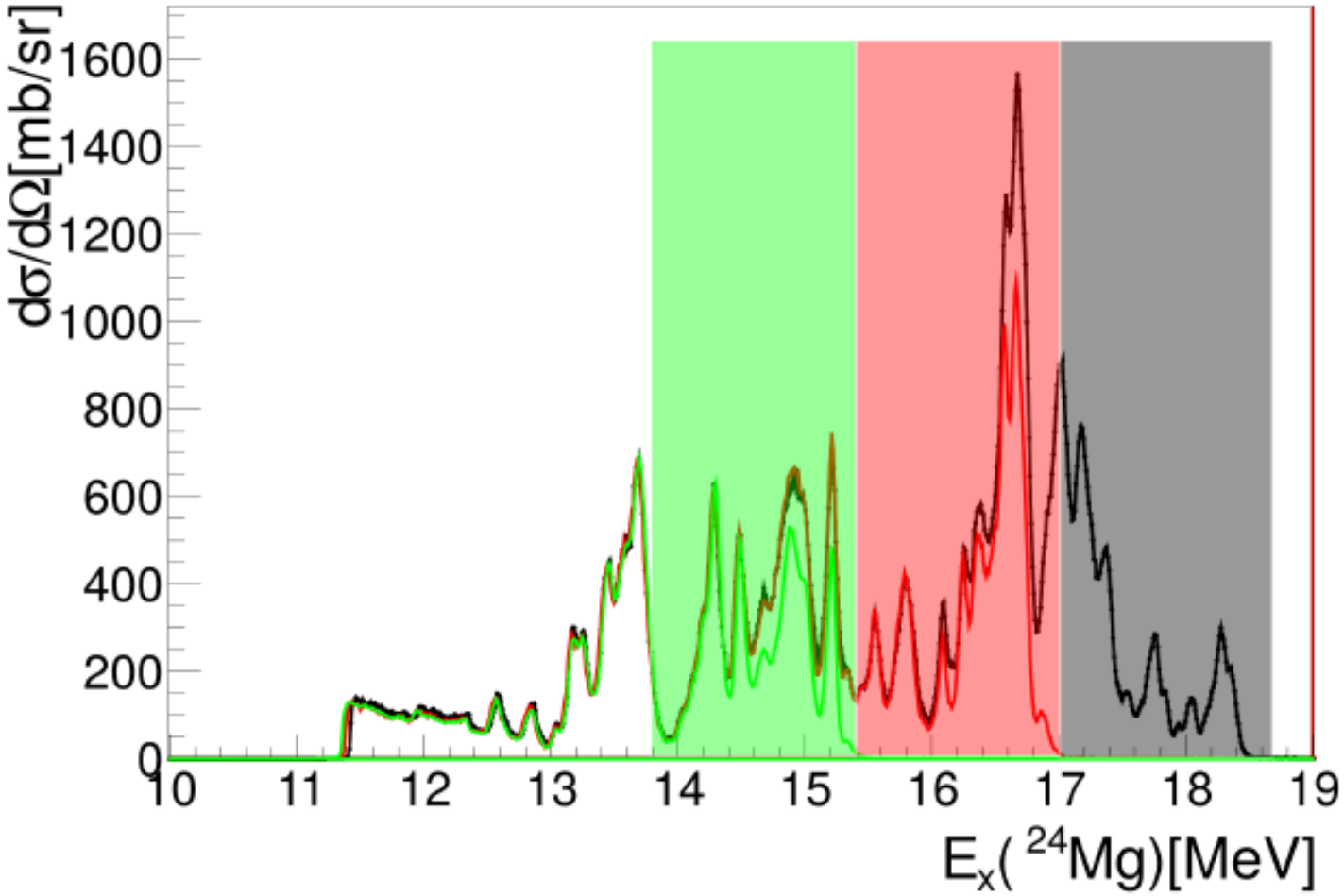

R-matrix fit

- code AZURE2: R. E. Azuma et al. Azure: An R-matrix code for nuclear astrophysics. Physical Review C 81 045805, (2010) 172
- input parameters: energies and partial widths of the states
- measurements of the $^{20}Ne(\alpha,\alpha_0)$ R. Abegg and C. A. Davis, Phys. Rev. C 43 6 (1991); ≈120 states between 12.5 and 18.5 MeV

- data taken for 16 angles in energy steps of 10 – 15 keV

Abegg & Davis spectrum at 168°

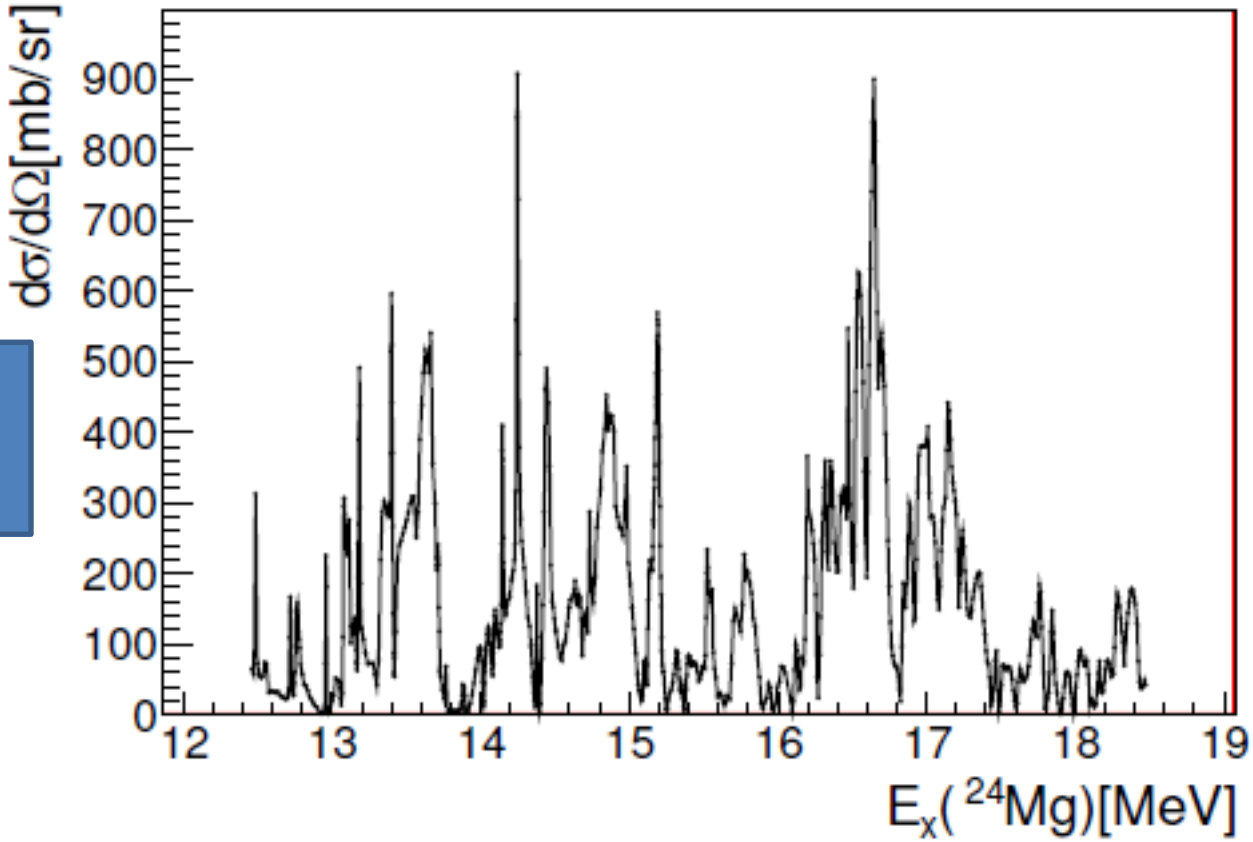

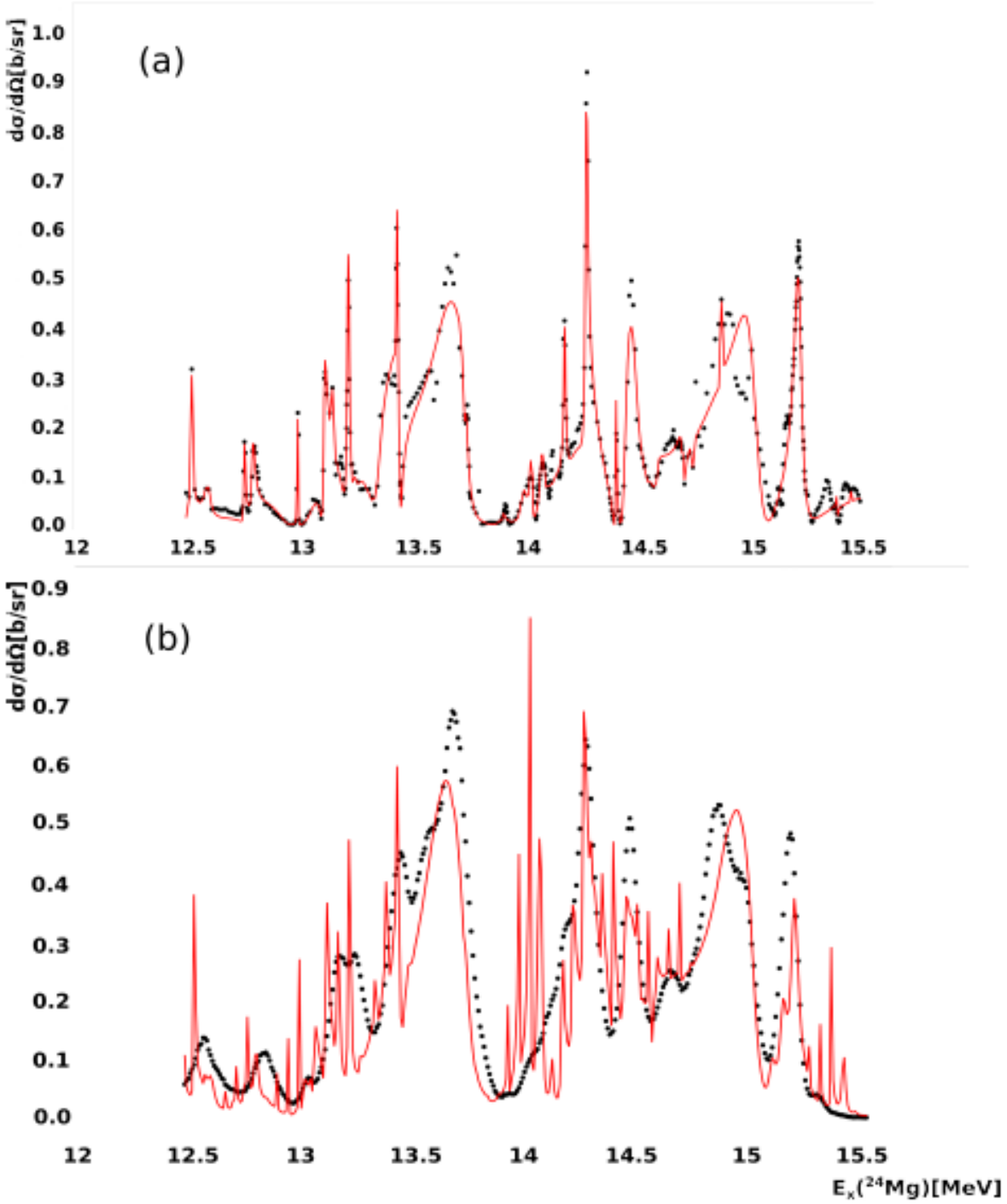

Abegg & Davis spectrum at 168°

Data for inelastic and proton channel included if improve the fit, energies and spin/parity fixed, partial widhts are free parameters, 52 states in this range

Tokić et al spectrum at 177° for E_{beam}=44 MeV convoluted by experimental resolution of 50 keV

- improved fit: all states with width < 10 keV excluded, energies and spin varied in limited range, inelastic-free part of the spectra only

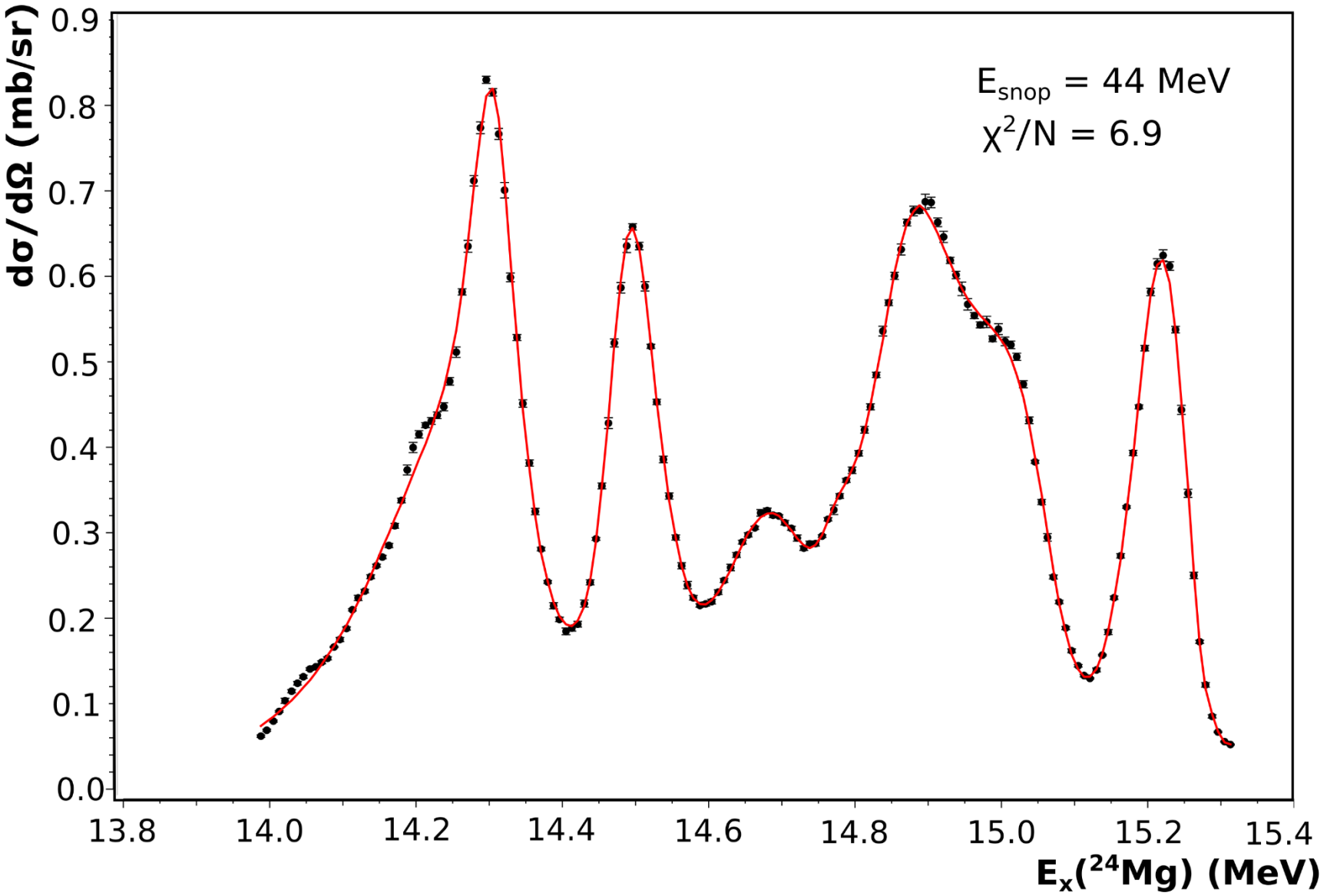

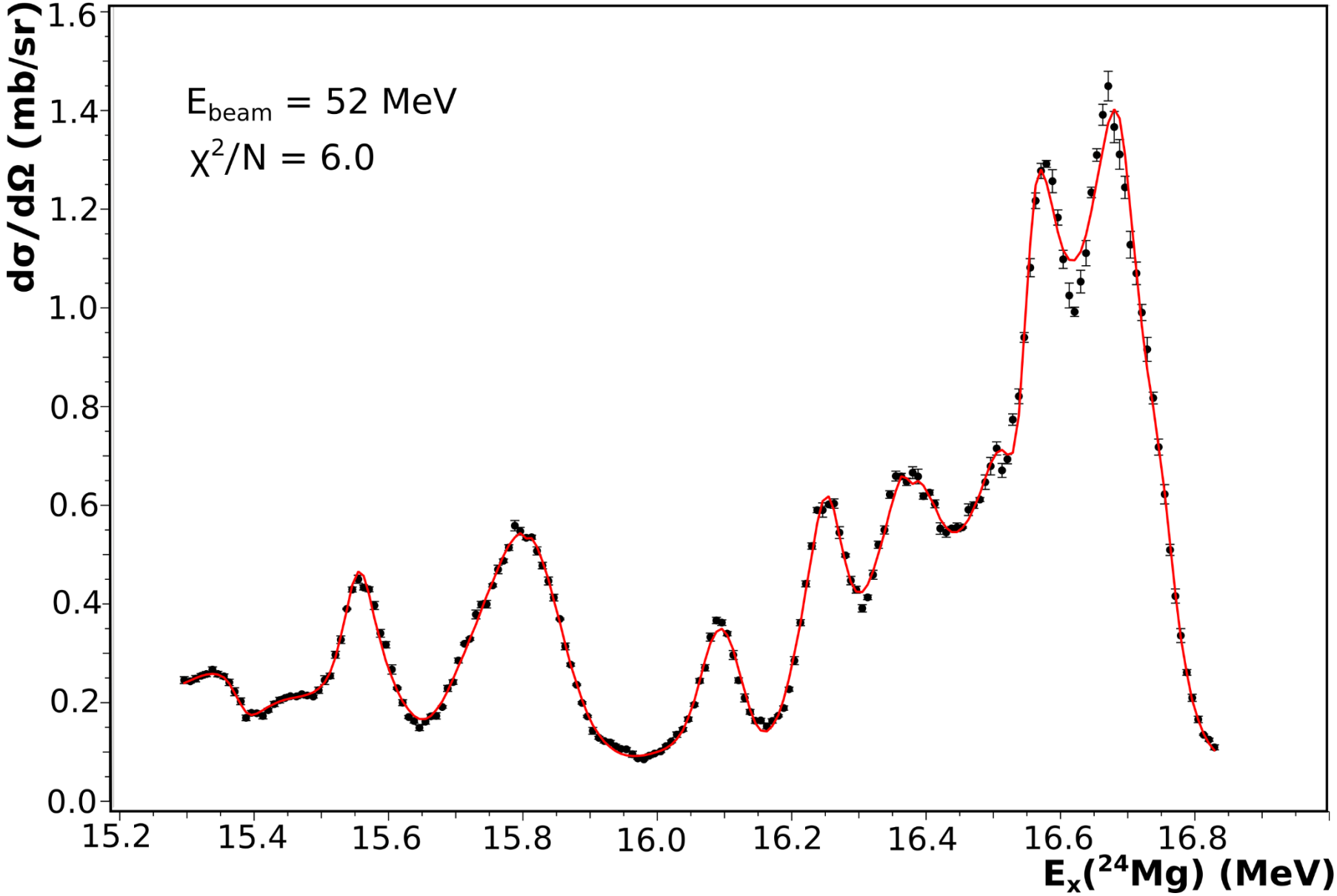
E_{beam} = 52 MeV
χ^2/N = 6.0
dσ/dΩ (mb/sr)
$E_x(^{24}Mg)$ (MeV)
0.0
0.2
0.4
0.6
0.8
1.0
1.2
1.4
1.6
15.2
15.4
15.6
15.8
16.0
16.2
16.4
16.6
16.8

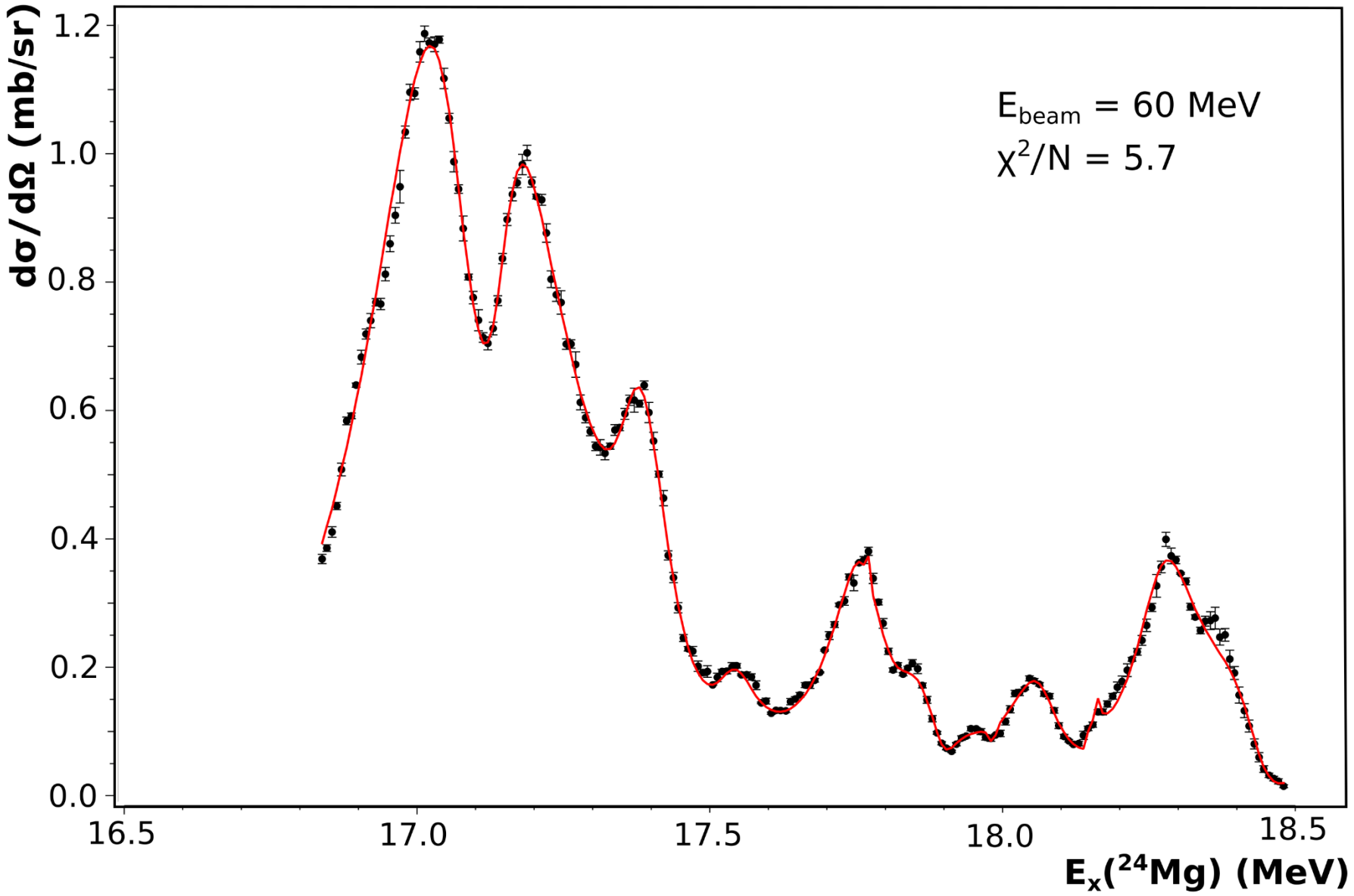
dσ/dΩ (mb/sr)
1.2
1.0
0.8
0.6
0.4
0.2
0.0
16.5
17.0
17.5
18.0
18.5
E_x(^24Mg) (MeV)
E_beam = 60 MeV
χ^2/N = 5.7

$E_x(^{24}Mg)$ (MeV)	J^π
14.016	1^-
14.296	4^+
14.470	3^-
14.485	4^+
14.674	2^+
14.686	3^-
14.700	5^-
14.766	4^+
14.884	1^-
14.891	2^+
14.938	1^-
15.079	4^+
15.236	4^+
15.292	4^+
15.306	2^+

$E_x(^{24}Mg)$ (MeV)	J^π
15.111	2^+
15.3723	4^+
15.543	2^+
15.553	6^+
15.637	4^+
15.806	4^+
15.833	4^+
16.040	2^+
16.115	3^-
16.234	4^+
16.375	2^+
16.378	4^+
16.382	6^+
16.410	4^+
16.553	6^+
16.563	4^+
16.751	5^-
16.783	4^+
16.818	6^+

$E_x(^{24}Mg)$	J^π	$E_x(^{24}Mg)$	J^π
15.416	4^+	18.154	7^-
16.970	5^-	18.288	5^-
17.057	7^-	18.445	6^+
17.097	6^+	18.625	3^-
17.130	6^+		
17.156	5^-		
17.331	6^+		
17.496	6^+		
17.509	2^+		
17.534	4^+		
17.574	5^-		
17.584	3^-		
17.769	6^+		
17.773	6^+		
17.859	4^+		
17.910	4^+		
17.984	5^-		
18.067	2^+		
18.152	6^+		

Spillane et al

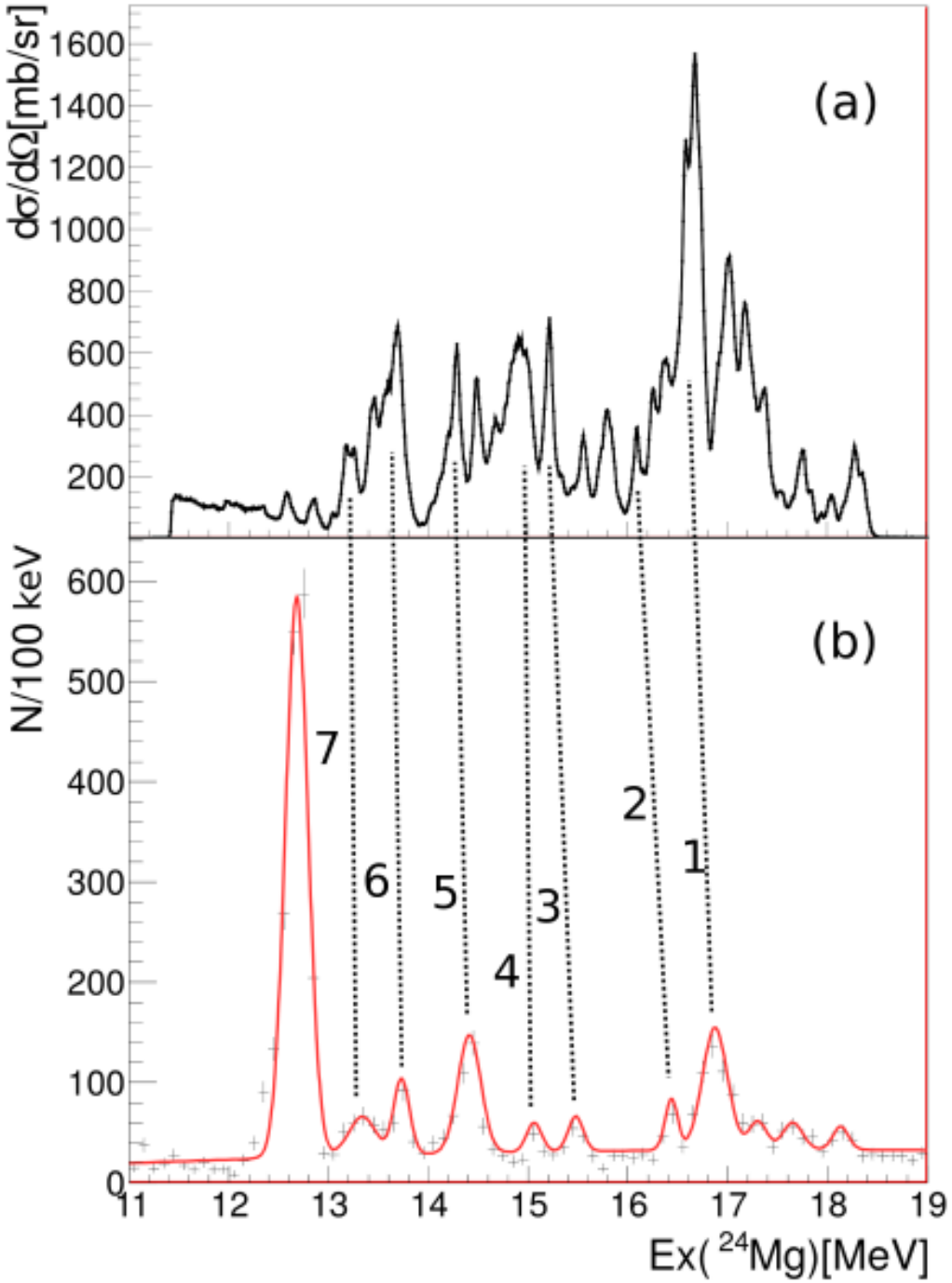

Excitation energy spectrum from Legnaro data for E_{beam}=60 MeV

Excitation energy spectrum from Catania data (≈200 keV off)

Recent experiment @LNL

8 DSSSD 1000 µm 5 x 5 cm^2

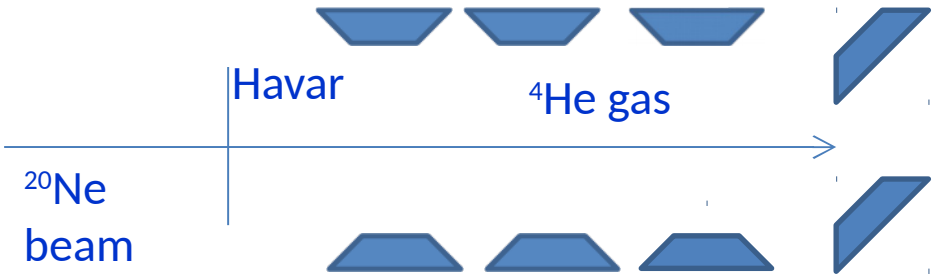

Beam energies: 48, 59 and 69 MeV - corresponding excitation energies in ^{24}Mg are 1.74, 3.72 and 5.50 MeV above the ^{12}C+^{12}C decay threshold.
Gas pressure (150 – 200 mbar) chosen to scan the ^{24}Mg excitation energy spectrum 1.74 →0.0, 3.72 → 1.5 and 5.50 → 3.5 MeV above the ^{12}C+^{12}C decay threshold.

Angular distributions measured in large CM angular range → essential to determine spin and parity by R-matrix calculations

- low gas pressure: at each beam energy the small range of the ^{24}Mg excitation energy will be scanned - much larger distance in the gas corresponds to the same excitation energy bin
- both scattered nuclei will be detected in coincidence - improved reconstruction of interaction point
- energy loss of α's negligible, energy loss of the ^{20}Ne will be calculated from reconstructed position of the interaction point

Largely improved energy resolution

- identification of the weak decay channels by kinematics

Summary

- a number of states decaying into ^{20}Ne+α at the ^{24}Mg excitations 14.0 - 18.6 MeV have been observed and characterized using R-matrix fit for the first time, but no $0^+/1^-$ state found in the Gamow window for the explosive ^{12}C+^{12}C burning
- two 1^- states observed at ≈14.9 MeV and the peak seen at the same excitation in the ^{12}C(^{16}O,αα)^{20}Ne data
- the 2^+ state observed at 16.04 MeV, possibly the same state is seen in the ^{12}C(^{16}O,αα)^{20}Ne – the last measured point in Spillane et al.
- limitations of experimental setup effect resonance characterization
- another approach: the ^{20}Ne+α resonant scattering with thin target & coincident detection of both collission products

THANK YOU !